Implementation of New Bias Correction Method for Aircraft Temperature with Kalman Filter in JMA's Global NWP System

NAKAMURA Yuki
Numerical Prediction Development Center, Japan Meteorological Agency
E-mail: yuki.nakamura@met.kishou.go.jp

1. Introduction

The Japan Meteorological Agency (JMA) utilizes meteorological data collected by commercial aircraft for assimilation into its global NWP system (GSM), and previously introduced correction for biases known to exist in such data (Ballish et al. 2008) for appropriate application (Sako 2010). Here, bias correction values were created and updated once a month using statistics from the previous month on the temperature first-guess departure from JMA's global data assimilation system. This was done separately for each aircraft and each vertical level, and bias correction values were used to correct aircraft temperature data for the next month. However, this approach was problematic from the perspective of effective use of aircraft temperature observations. For instance, update frequency was insufficient and aircraft temperature data were used without bias correction if there were insufficient data to enable calculation of correction values. Accordingly, a new bias correction method designed to solve these problems was implemented into operation after determination of its effectiveness with the GSM.

2. New bias correction

Other NWP centers use variational correction to correct aircraft temperature bias (Zhu et al. 2015). As this exerts a high computational cost on JMA's NWP system, Kalman filtering is applied for correction at much lower cost. Bias correction values are updated at each analysis time (0000, 0600, 1200, 1800 UTC) and calculated for processing independent of analysis using a covariance of the first-guess departure separately for each aircraft, each vertical level and each flight phase (ascent, cruising and descent). Kalman filtering involves prediction and updating. In the prediction step, the estimated bias correction value $\widehat{\boldsymbol{\beta}}$, the covariance $\mathbf{P}$ and the covariance of the first-guess departure $\mathbf{D}$ are developed from time $k-1$ to time k as follows:

$$\widehat{\boldsymbol{\beta}}^{-}(k) = \widehat{\boldsymbol{\beta}}(k-1) \quad (1)$$

$$\mathbf{P}^{-}(k) = \mathbf{P}(k-1) + \mathbf{U} \quad (2)$$

$$\mathbf{D}^{-}(k) = \mathbf{D}(k-1) \quad (3)$$

The superscript "−" represents a priori estimation, and $\mathbf{U}$ is equivalent to the covariance of system noise. Subsequently, $\widehat{\boldsymbol{\beta}}$, $\mathbf{P}$ and $\mathbf{D}$ are updated using the average first-guess departure $\mathbf{b}$ for each analysis at the update step. The relevant formulas are shown below.

$$\widehat{\boldsymbol{\beta}}(k) = \widehat{\boldsymbol{\beta}}^{-}(k) + \mathbf{G}\left(\mathbf{b}(k) - \widehat{\boldsymbol{\beta}}^{-}(k)\right) \quad (4)$$

$$\mathbf{P}(k) = (\mathbf{I} - \mathbf{G})\mathbf{P}^{-}(k) \quad (5)$$

$$\mathbf{D}(k) = r\mathbf{D}^{-}(k) + (1-r)\left[\mathbf{b}(k) - \widehat{\boldsymbol{\beta}}^{-}(k)\right]^2 \quad (6)$$

$$\mathbf{G} = \frac{\mathbf{P}^{-}(k)}{\mathbf{P}^{-}(k) + \mathbf{D}(k)} \quad (7)$$

Here, $\mathbf{G}$ is the Kalman gain, r is the update ratio for $\mathbf{D}$, and $\mathbf{U}$ and r are unique values based on pre-runs of the new bias correction method. Evaluation using past observation and GSM data indicated that the new method enables calculation of more suitable bias correction values than the conventional approach (Figure 1).

3. Verification and results

To verify the influence of the new bias correction on the GSM, observing system experiments were performed as per the operational GSM on August 27 2020 (CNTL) and with the new bias correction method (TEST) for the experimental periods of August 2019 and January 2020. Initial bias correction values for TEST were created via Kalman filtering for the previous two years using first-guess departures.

The results indicated highly appropriate correction of aircraft temperature biases against first guesses with the new approach (Figure 2). Figure 3 (left) also shows that biases of aircraft temperature against first guesses were reduced. Biases of first-guess temperature against radiosonde observations were also reduced, especially around 250 hPa (Figure 3, right). Focusing on horizontal temperature distribution averaged over the experimental period, the temperature analysis field around 250 hPa in TEST was globally cooler than in CNTL (Figure 4). In terms of forecast accuracy, root mean squared errors of temperature and geopotential height against radiosondes and analysis were reduced in comparison with CNTL (Figure 5). The experimental results were consistent for both August 2019 and January 2020, and tropical cyclone track forecast error statistics were similar between TEST and CNTL. However, track forecast errors were improved for some tropical cyclones. These improvements are attributable to improved forecast accuracy of geopotential height in TEST.

As the new bias correction method demonstrated better performance than the conventional approach, it was implemented into JMA's global NWP system in June 2021.

References

Ballish, B. A., and K. Kumar, 2008: Systematic differences in aircraft and radiosonde temperatures. *Bull. Amer. Meteor. Soc.*, **89**, 1689-1708.

Sako, H., 2010: Assimilation of Aircraft Temperature Data in the JMA Global 4D-Var Data Assimilation System. *WGNE. Res. Activ. Earth. Sys. Modell.*, **40**, 1.33-1.34.

Zhu, Y., J. C. Derber, R. J. Purser, B. A. Ballish, and J. Whiting, 2015: Variational Correction of Aircraft Temperature Bias in the NCEP's GSI Analysis System. *Mon. Wea. Rev.*, **143**, 3774–3803.

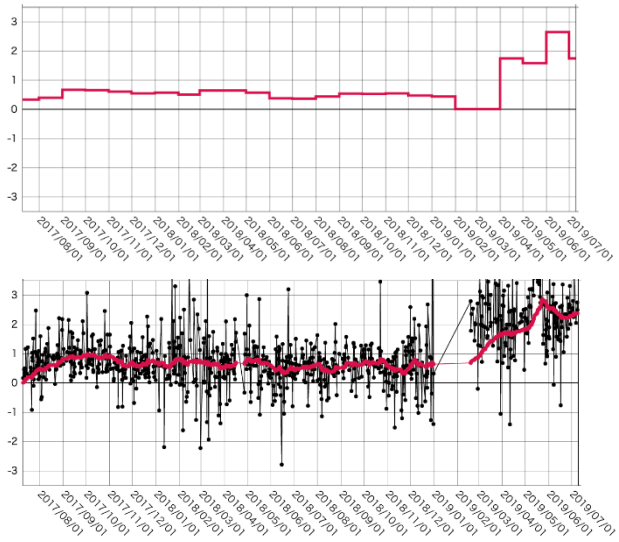

Figure 1. Time-series representation of bias correction values (red) for aircraft observation temperatures at around 200 hPa from July 10, 2017 to July 9, 2019. The top and bottom figures show values calculated using the conventional and new methods, respectively. The black line represents averaged first-guess departures at each analysis time. The unit is K.

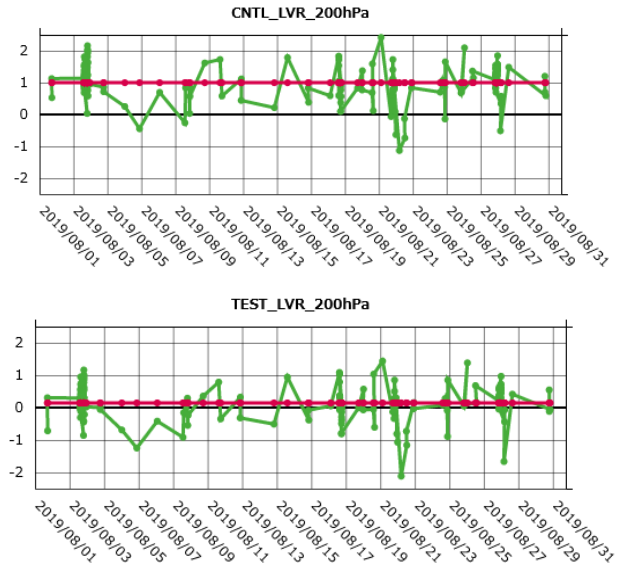

Figure 2. Time-series representation of first-guess departures of temperature [K] in aircraft observation around 200 hPa in August 2019. The green line represents first-guess departures at each analysis time, and the red line shows values averaged over the experimental period. The top and bottom figures show CNTL and TEST, respectively.

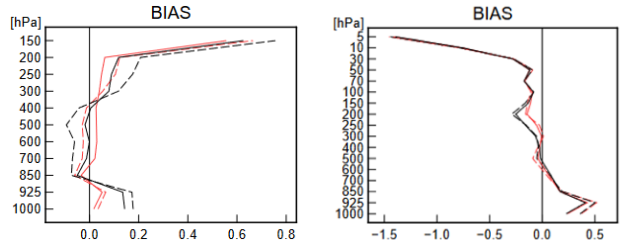

Figure 3. Temperature bias [K] in aircraft (left) and radiosonde (right) data against first guesses (dashed line) and analysis (solid line) at each vertical level for CNTL (black) and TEST (red) in August 2019. These biases were calculated only with data used in assimilation.

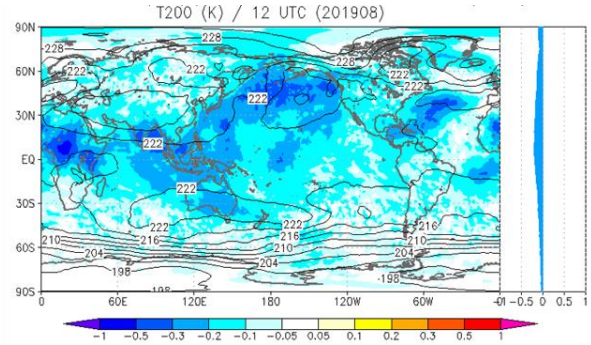

Figure 4. Average difference of horizontal temperature distribution at 200 hPa for the experimental period in August 2019 (only 1200 UTC) between TEST and CNTL. The zonal mean is also shown on the right. The unit is K.

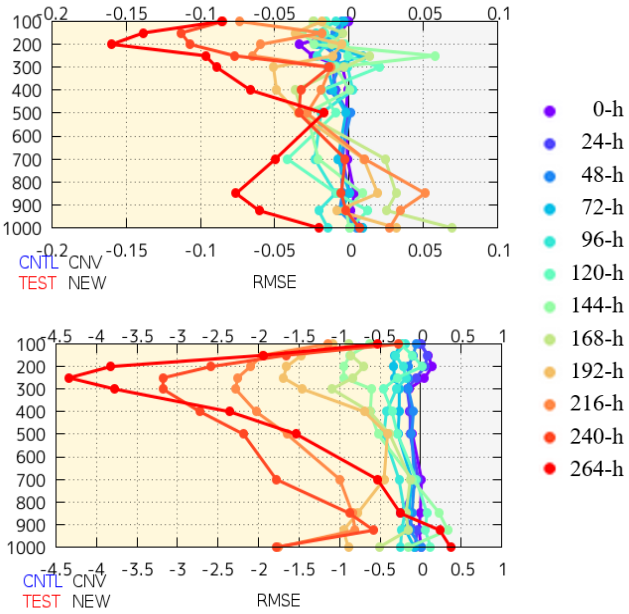

Figure 5. Differences in root mean square errors between TEST and CNTL against radiosondes averaged over the experimental period at each vertical level in the Northern Hemisphere in August 2019. The top and bottom figures show temperature [K] and geopotential height [m] forecasts, respectively, and colors represent each forecast time. The yellow area represents improvement because of reduced root mean square errors.